Supplement of Atmos. Chem. Phys., 23, 14919–14932, 2023
https://doi.org/10.5194/acp-23-14919-2023-supplement

Supplement of

Insights into soil NO emissions and the contribution to surface ozone formation in China

Ling Huang et al.

Correspondence to: Li Li (lily@shu.edu.cn)

Section S1: Details of the BDSNP algorithm

Biome-specific emission factor

$$A'_{biome} = A_{biome} + N_{avail} \times E \qquad \text{Eq. S1}$$

Temperature and soil moisture dependence factor

$$\mathrm{f(T)} = e^{k[^{\circ}\mathrm{C}^{-1}]T} \qquad k = 0.103 \pm 0.04 \qquad \text{Eq. S2}$$

$$\mathrm{g}(\theta) = \mathrm{a}\theta e^{-b\theta^2} \qquad \text{Eq. S3}$$

Pulsing

$$P(l_{dry}, t) = [13.01 \ln(l_{dry}) - 53.6] \times e^{-ct} \qquad c = 0.068\ \mathrm{h}^{-1} \qquad \text{Eq. S4}$$

P represents the magnitude of the peak flux relative to the pre-wetting flux, and the constant c is a rate constant representing the rise/fall time of the pulse. The value of l_{dry} is the antecedent dry period in hours.

Soil N content

$$N_{avail}(t) = N_{avail}(0)e^{-t/\tau} + F \times \tau \times (1 - e^{-t/\tau}) \qquad \text{Eq. S5}$$

where N_{avail} is the mass of available N in the soil (ng N m^{-2}), F is the application rate, and τ is a decay lifetime.

Table S1 Division of regions.

Region	Provinces
Northeast China	Liaoning, Heilongjiang, Jilin
North China	Hebei, Inner Mongolia, Tianjin, Beijing, Shanxi
Central China	Henan, Hubei, Hunan
East China	Fujian, Jiangsu, Shandong, Zhejiang, Shanghai, Anhui, Jiangxi
South China	Hainan, Guangdong, Guangxi
Southwest China	Tibet, Sichuan, Yunnan, Chongqing, Guizhou
Northwest China	Xinjiang, Qinghai, Gansu, Ningxia, Shaanxi

Table S2 Differences of fertilizer applied between the default dataset and the statistical yearbook.

Province/ Region	Amount of nitrogen fertilizer from Potter's dataset (Tg N)	Statistical yearbook for year 2018			Relative difference (%)
		Amount of pure nitrogen fertilizer (Tg N)	Amount of NPK compound fertilizer (Tg N)	Total (pure nitrogen fertilizer + 1/3 NPK fertilizer) (Tg N)	
Gansu	0.48	0.33	0.27	0.42	-13.7
Ningxia	0.12	0.16	0.15	0.21	45.6
Qinghai	0.11	0.03	0.03	0.05	-146.7
Shaanxi	0.59	0.89	0.99	1.22	51.2
Xinjiang	0.40	1.10	0.59	1.30	68.8
Northwest China	***1.71***	***2.52***	***2.03***	***3.19***	***46.6***
Henan	1.58	2.02	3.37	3.14	49.7
Hubei	0.91	1.13	1.08	1.49	38.6
Hunan	0.95	0.94	0.81	1.21	21.4
Central China	***3.45***	***4.09***	***5.26***	***5.84***	***41.0***
Guizhou	0.63	0.40	0.30	0.50	-25.5
Sichuan	1.28	1.12	0.60	1.32	3.2
Tibet	0.19	0.01	0.02	0.02	-728.3
Yunnan	0.74	1.05	0.56	1.24	40.5

Chongqing	0.46	0.46	0.25	0.54	14.8
Southwest China	***3.30***	***3.05***	***1.74***	***3.63***	***9.1***
Guangdong	0.75	0.89	0.71	1.12	33.3
Guangxi	0.84	0.74	0.95	1.06	20.4
Hainan	0.13	0.15	0.22	0.22	41.7
South China	***1.72***	***1.77***	***1.88***	***2.40***	***28.4***
Anhui	1.03	0.96	1.60	1.49	30.7
Fujian	0.34	0.42	0.31	0.52	35.5
Jiangsu	0.97	1.46	0.96	1.77	45.5
Jiangxi	0.67	0.34	0.53	0.52	-29.9
Shandong	1.45	1.31	2.12	2.01	27.8
Shanghai	0.08	0.04	0.04	0.05	-64.2
Zhejiang	0.48	0.40	0.23	0.48	0.0
East China	***5.02***	***4.92***	***5.79***	***6.85***	***26.7***
Beijing	0.09	0.03	0.03	0.04	-106.6
Hebei	1.15	1.14	1.50	1.64	29.8
Inner Mongolia	0.74	0.86	0.77	1.12	33.6
Shanxi	0.48	0.25	0.64	0.47	-2.6
Tianjin	0.05	0.06	0.08	0.08	40.7

North China	***2.51***	***2.35***	***3.03***	***3.35***	***25.2***
Heilongjiang	0.86	0.84	0.78	1.10	21.3
Jilin	0.51	0.58	1.50	1.08	52.8
Liaoning	0.53	0.55	0.68	0.78	31.9
Northeast China	***1.90***	***1.97***	***2.96***	***2.95***	***35.6***
Total	19.60	20.65	22.69	28.22	30.5

Table S3 Model configurations of WRF and CAMx.

Items	WRF	CAMx
Version	3.7	7.0
Gas-Phase chemistry		Carbon Bond chemistry (CB6) (Yarwood et al., 2010)
Aerosol module		CF Scheme / ISORROPIA
Aqueous-phase chemistry		Updated mechanism of the Regional Acid Deposition Model (RADM) (Chang et al., 1987)
Planet boundary scheme	The Yonsei University Scheme (YSU) (Hong et al., 2006)	
Land surface	NOAH (Ek et al., 2003)	
Microphysics	Morrison double-moment scheme (Morrison et al., 2009)	
Shortwave radiation	RRTMG shortwave (Iacono et al., 2008)	
Longwave radiation	RRTMG scheme (Iacono et al., 2008)	
Boundary conditions / initial conditions	1°×1° grids FNL Operational Global Analysis data archived at the GDAS	MOZART (Emmons et al., 2010)
Dry deposition and wet deposition		Zhang et al. (2003)

Table S4 Statistical index formula.

No.	Index	Formula	Note
1	Pearson correlation coefficient (R)	$\frac{\sum[(P_j-\overline{P})\times(O_j-\overline{O})]}{\sqrt{\sum(P_j-\overline{P})^2\times\sum(O_j-\overline{O})^2}}$	Unitless, -1≤R≤1
2	mean bias (MB)	$\frac{\sum(P_j-O_j)}{N}$	concentration unit
3	root-mean-square error (RMSE)	$\sqrt{\frac{\sum(P_j-O_j)^2}{N}}$	concentration unit
4	normalized mean bias (NMB)	$\frac{\sum(P_j-O_j)}{\sum O_j}\times 100$	-100%≤NMB≤+∞
5	normalized mean error (NME)	$\frac{\sum\lvert P_j-O_j\rvert}{\sum O_j}\times 100$	0%≤NME≤+∞

Table S5 Soil NO emissions* and ratio of soil NO to anthropogenic NO_x by different regions in China for 2018.

Region	Annual Soil NO emissions (Gg)	Soil NO emissions during June-August (Ratio of annual totals)	Ratio of soil NO/anthropogenic NO_x	Ratio soil NO/anthropogenic NO_x (June-August)
Northeast China	94.2	63.7 (67.6%)	12.0%	36.0%
North China	200.5	118.1 (58.9%)	14.9%	36.5%
Central China	281.4	146.7 (52.1%)	35.3%	74.0%
East China	264.3	138.4 (52.4%)	12.8%	26.8%
South China	71.4	20.1 (28.2%)	14.3%	15.8%
Southwest China	87.6	34.8 (39.7%)	14.5%	23.9%
Northwest China	158.4	95.8 (60.5%)	26.8%	67.5%
Total	1157.9	617.6 (53.3%)	17.3%	37.9%

*Soil NO emissions given in this table are based on the default temperature dependence factor.

Table S6 Comparison of observed and simulated values in China and five key regions.

	China	**NCP**	**YRD**	**PRD**	**Sichuan Basin**	**Northeast**
OBS (μg/m^3)	129.6	172.4	146.5	97.5	108.3	126.1
MOD (μg/m^3)	146.7	185.7	171.5	108.4	146.7	128.4
MB (μg/m^3)	17.1	13.3	25.0	10.9	38.5	2.4
NMB (%)	13.2	7.7	17.1	11.2	35.5	1.9
R	0.89	0.77	0.80	0.58	0.62	0.83

Table S7 Comparison of soil NO emissions and flux in China reported by previous studies.

Reference	Region	Reference year	Above canopy (Gg N a^{-1})	Soil NO_x flux (ng N m^{-2} s^{-1})	Notes
Wang et al. (2005)	China	1999	657	generally more than 40 ng N m^{-2} s^{-1} (in the North China Plain in July) and 20 ng N m^{-2} s^{-1} (in the northeast China in July)	An empirical modeling approach of Yienger and Levy (YL95)
Tie et al. (2006)	China	2004	1375		Dynamical and biogenic emissions models, soil emissions parameterized with an exponential dependence on soil temperature.
Yan et al. (2005)	China		480		Statistical model based on field measurements of NO_x fluxes combined with land cover, soil pH, soil organic carbon, climate, and nitrogen fertilizers
Huang and Li (2014)	China		1226 (ranging from 588.24 to 2132.05)		Synthesis of 130 NO emissions sampling points at 14 locations to estimate soil NO emissions inventory in China.
Lu et al. (2019)	China	2016 (Mar-Oct)	1140		BDSNP scheme in GEOS-Chem
		2017 (Mar-Oct)	1360		

Lu et al. (2021)	China	2017	770±40		BDSNP scheme in GEOS-Chem
Wang et al. (2007)	East China	1997-1999	850		Application of YL95 scheme in GEOS-Chem
Lin (2012)	East China	2006	380		Top-down estimates using satellite NO_2 retrievals
Wang et al. (2022)	The North China plain	2020		10-40 (crop growing season)	Application of MEGAN scheme in WRF-Chem
Li and Wang (2007)	the Pearl River Delta	2005		The average is 47.5 (typical vegetable plot)	NO flux measured by static chamber technique in the suburbs of Guangzhou
Li et al. (2007)	South China	2005		The average fluxes of broadleaved forest and pine-leaved forest in the rainy season were 14.9 and 17.1	Sample plots circled in the forest and NO fluxes measured by dynamic flow chamber technique
Liu et al. (2011)	Northern China	2007-2009		Average annual flux of 7.6 (wheat-maize rural)	Experiments NO fluxes were obtained based on automatic measurement systems and intermittent manual measurements
Liu et al. (2017)				The average soil NO flux was 12.9 Vegetable farmland flux is 30.9	Synthesized 520 field observations from 114 publications
This study	China	2018	805.2	6.6 (June average, same below)	BDSNP scheme (default fertilizer data)
			1157.9 (715.7-1902.6)	9.9	BDSNP scheme (N + compound fertilizer data)

		296.1	38.5	BDSNP scheme (default fertilizer data)
NCP	2018	455.9 (276.5-762.1)	60.1	BDSNP scheme (N + compound fertilizer data)
			35.4	BDSNP scheme (N + compound fertilizer data and adjusted β value)

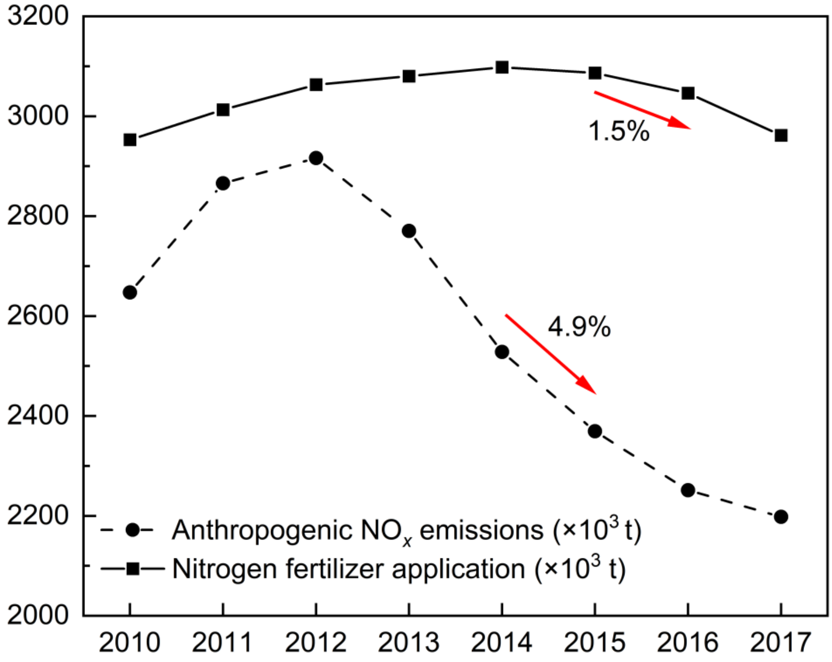

Figure S1: Anthropogenic NO_x emissions and nitrogen fertilizer application during 2010—2017 (Note: anthropogenic NO_x emissions are based on MEIC emission inventory; nitrogen fertilizer data from provincial statistical yearbook).

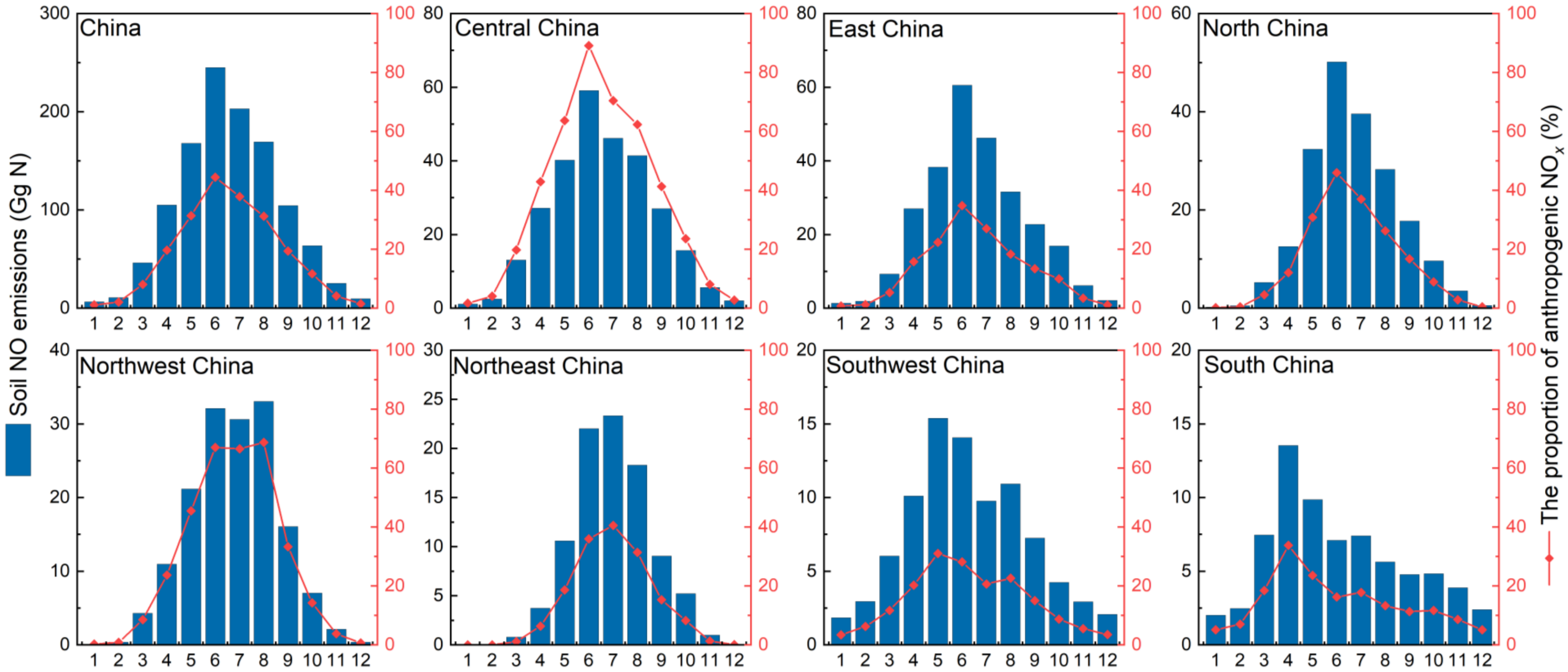

Figure S2: Monthly soil NO emissions (estimated with default temperature dependence factor of 0.103) by region.

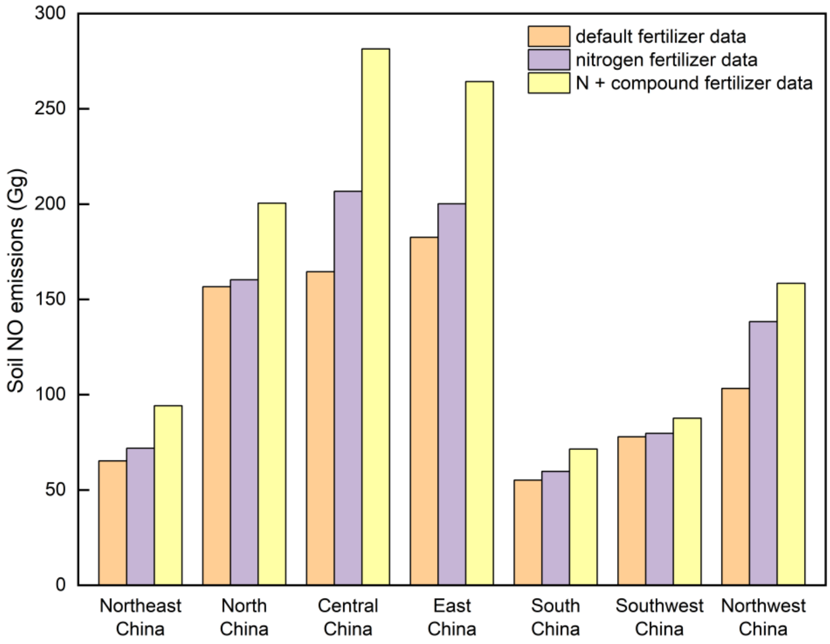

Figure S3: Soil NO emissions estimated using different fertilizer data (default fertilizer data: International Fertilizer Industry Association from Potter et al. (2010) for year 2010; nitrogen fertilizer and compound fertilizer are from statistical yearbooks at the provincial level for year 2018).

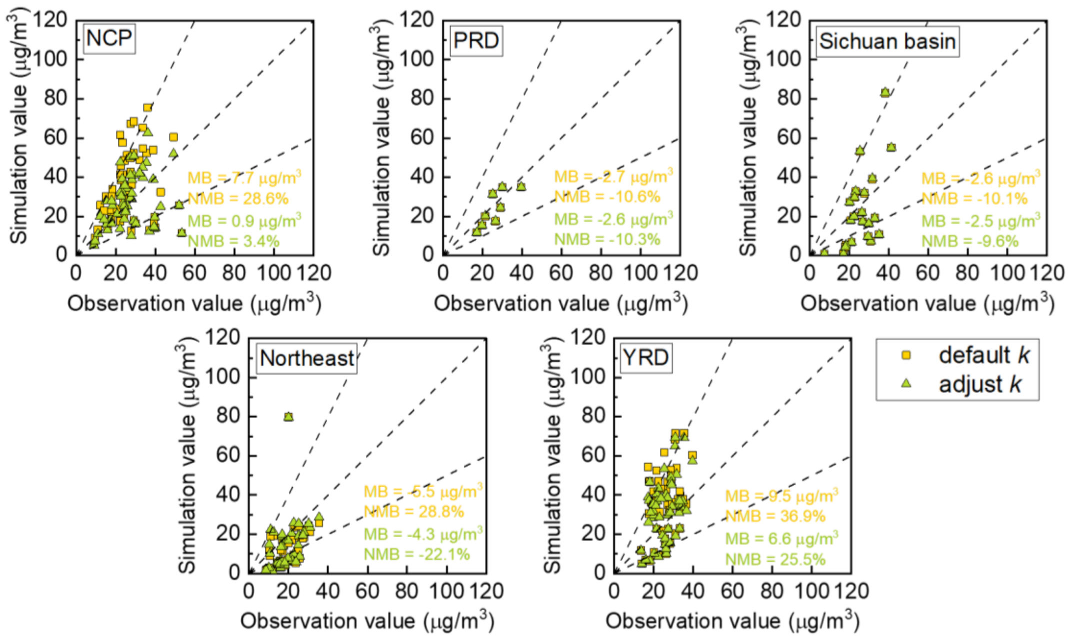

Figure S4: Scatter plot of monthly mean NO_2 concentration (before and after adjusting *k*).

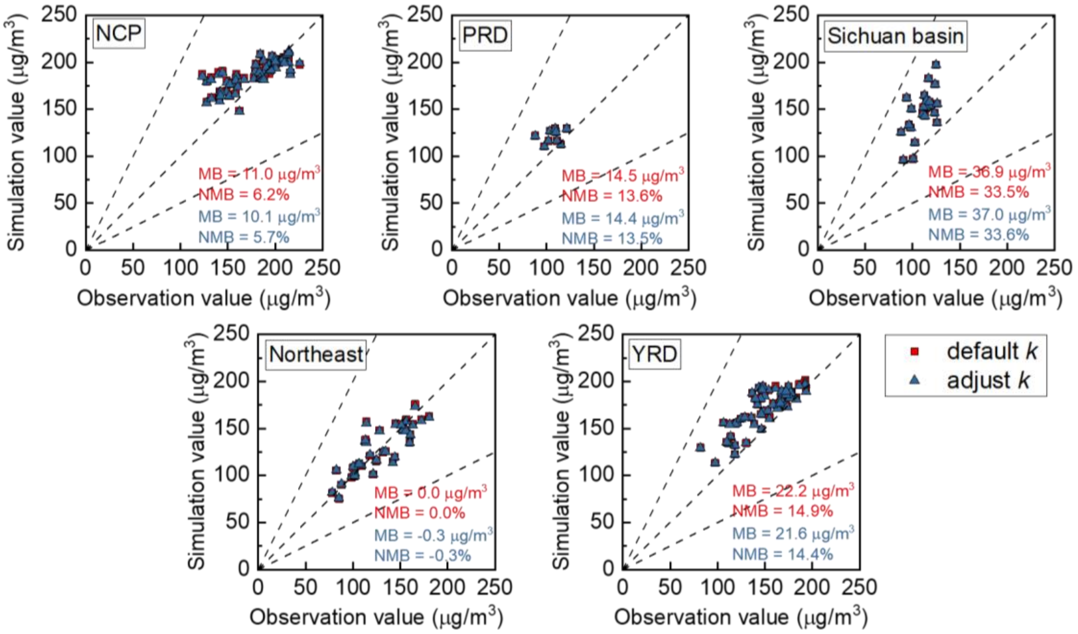

Figure S5: Scatter plot of monthly mean MDA8 ozone concentration (before and after adjusting *k*).

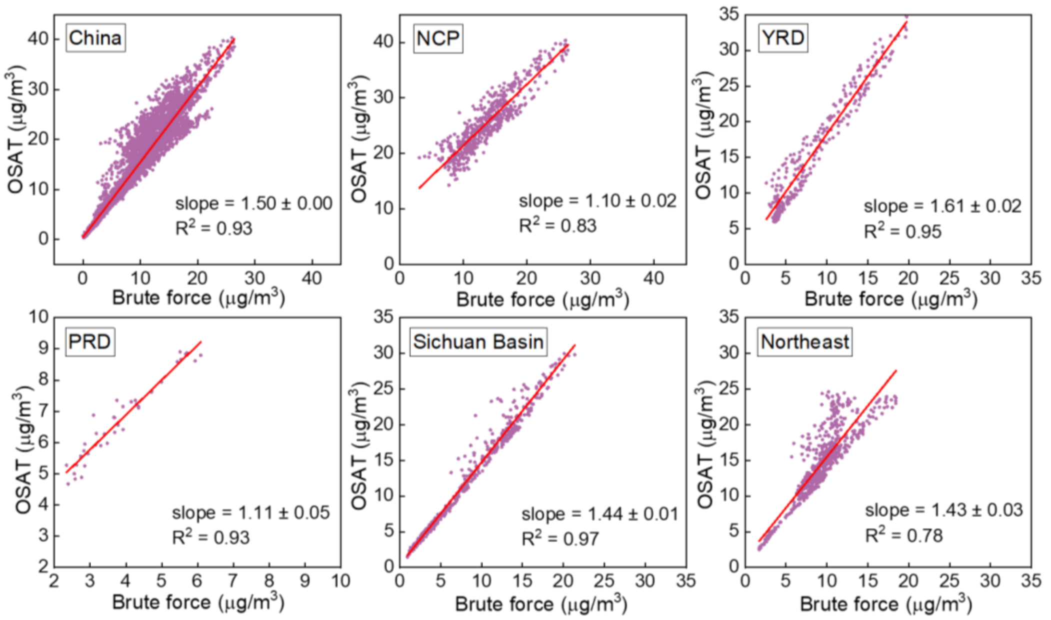

Figure S6: Comparison of OSAT method and Brute force method in China and five key regions.

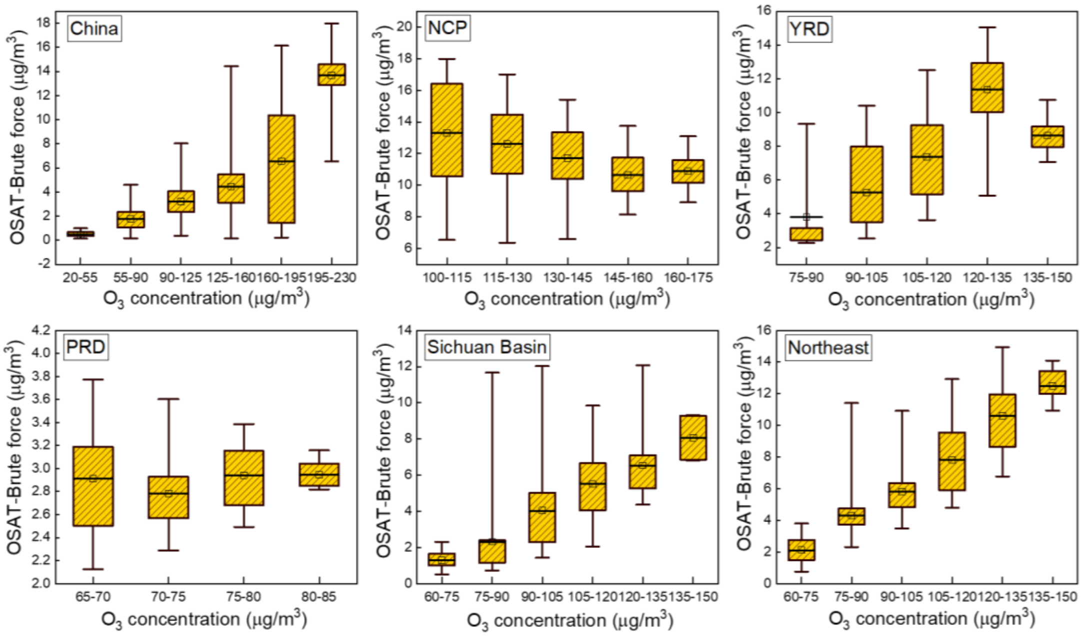

Figure S7: Ozone differences between OSAT method and brute force method under different ozone concentrations in China and five key regions.

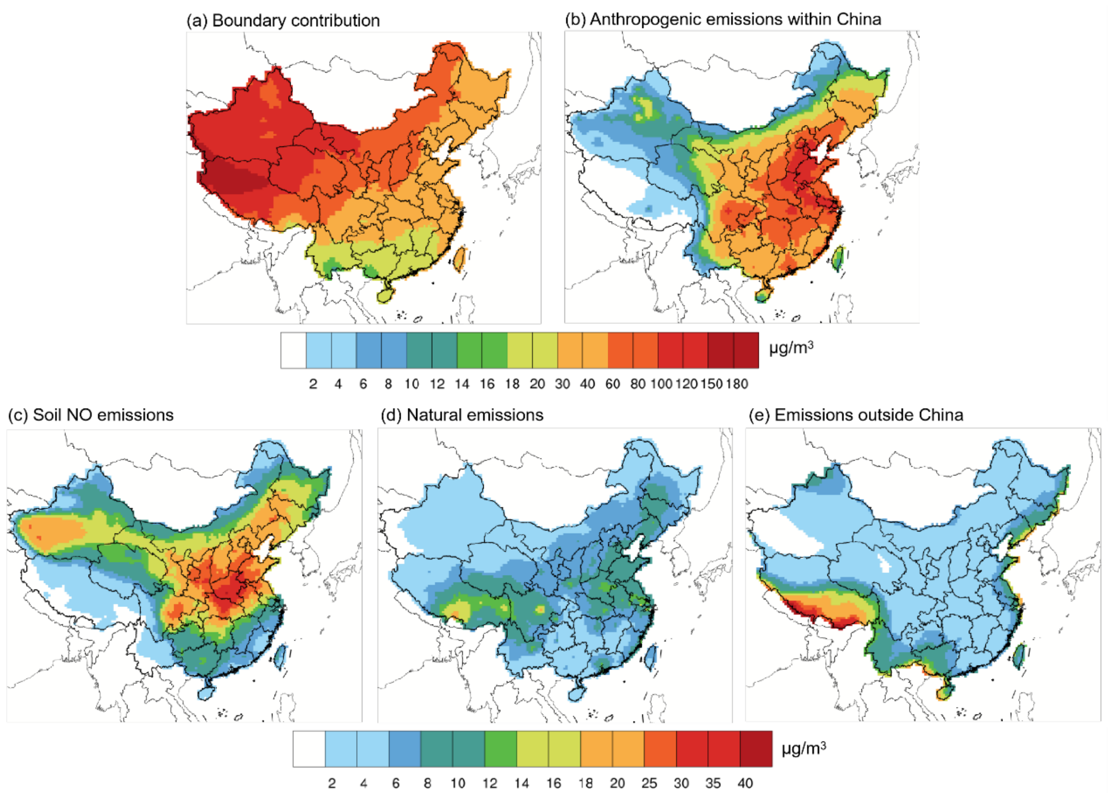

Figure S8: Spatial distribution of ozone contribution from different source groups based on OSAT results.

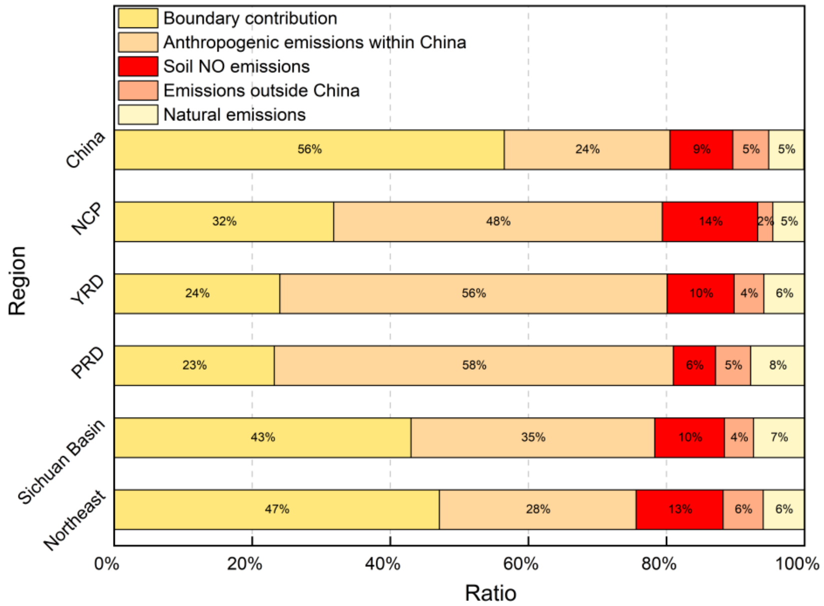

Figure S9: Relative ozone contribution by emission groups and regions.

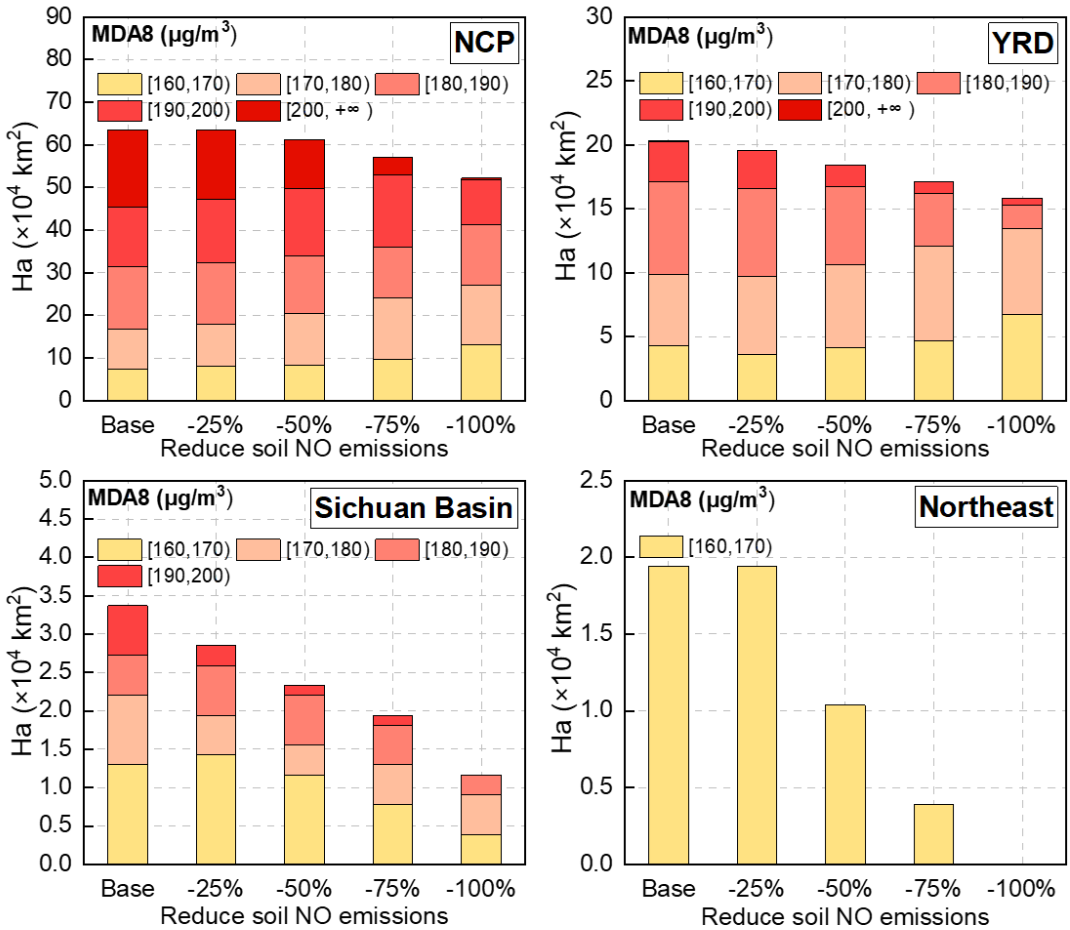

Figure S10: Area exposed to MDA8 > 160 μg/m^3 under different soil NO emission reduction scenarios (PRD is not shown because MDA8 ozone concentration is less than 160 μg/m^3).

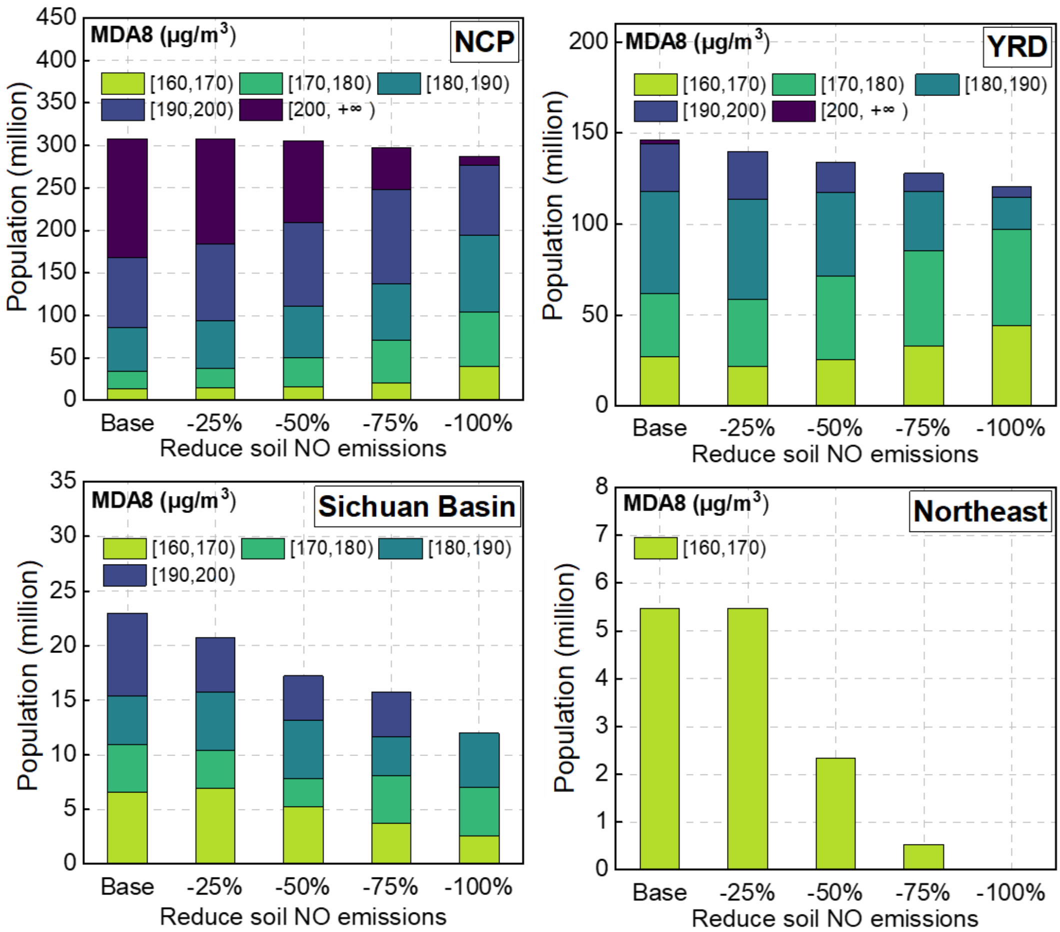

Figure S11: Population exposed to MDA8 > 160 μg/m^3 under different soil NO emission reduction scenarios (PRD is not shown because MDA8 ozone concentration is less than 160 μg/m^3).

References:

Chang, J., Brost, R., Isaksen, I., Madronich, S., Middleton, P., Stockwell, W., and Walcek, C.: A three-dimensional Eulerian acid deposition model: Physical concepts and formulation, Journal of Geophysical Research: Atmospheres, 92, 14681-14700, 1987.

Ek, M., Mitchell, K., Lin, Y., Rogers, E., Grunmann, P., Koren, V., Gayno, G., and Tarpley, J.: Implementation of Noah land surface model advances in the National Centers for Environmental Prediction operational mesoscale Eta model, Journal of Geophysical Research: Atmospheres, 108, 2003.

Emmons, L. K., Walters, S., Hess, P. G., Lamarque, J.-F., Pfister, G. G., Fillmore, D., Granier, C., Guenther, A., Kinnison, D., and Laepple, T.: Description and evaluation of the Model for Ozone and Related chemical Tracers, version 4 (MOZART-4), Geoscientific Model Development, 3, 43-67, 2010.

Hong, S.-Y., Noh, Y., and Dudhia, J.: A new vertical diffusion package with an explicit treatment of entrainment processes, Monthly weather review, 134, 2318-2341, 2006.

Huang, Y. and Li, D.: Soil nitric oxide emissions from terrestrial ecosystems in China: a synthesis of modeling and measurements, Scientific Reports, 4, 1-8, 2014.

Iacono, M. J., Delamere, J. S., Mlawer, E. J., Shephard, M. W., Clough, S. A., and Collins, W. D.: Radiative forcing by long-lived greenhouse gases: Calculations with the AER radiative transfer models, Journal of Geophysical Research: Atmospheres, 113, 2008.

Li, D. and Wang, X.: Nitric oxide emission from a typical vegetable field in the Pearl River Delta, China, Atmospheric Environment, 41, 9498-9505, 2007.

Li, D., Wang, X., Mo, J., Sheng, G., and Fu, J.: Soil nitric oxide emissions from two subtropical humid forests in south China, Journal of Geophysical Research: Atmospheres, 112, 2007.

Lin, J.-T.: Satellite constraint for emissions of nitrogen oxides from anthropogenic, lightning and soil sources over East China on a high-resolution grid, Atmospheric Chemistry and Physics, 12, 2881-2898, 2012.

Liu, C., Wang, K., Meng, S., Zheng, X., Zhou, Z., Han, S., Chen, D., and Yang, Z.: Effects of irrigation, fertilization and crop straw management on nitrous oxide and nitric oxide emissions from a wheat–maize rotation field in northern China, Agriculture, Ecosystems & Environment, 140, 226-233, 2011.

Liu, S., Lin, F., Wu, S., Ji, C., Sun, Y., Jin, Y., Li, S., Li, Z., and Zou, J.: A meta-analysis of fertilizer-induced soil NO and combined NO+ N2O emissions, Global Change Biology, 23, 2520-2532, 2017.

Lu, X., Ye, X., Zhou, M., Zhao, Y., Weng, H., Kong, H., Li, K., Gao, M., Zheng, B., and Lin, J.: The underappreciated role of agricultural soil nitrogen oxide emissions in ozone pollution regulation in North China, Nature communications, 12, 5021, 2021.

Lu, X., Zhang, L., Chen, Y., Zhou, M., Zheng, B., Li, K., Liu, Y., Lin, J., Fu, T.-M., and Zhang, Q.: Exploring 2016–2017 surface ozone pollution over China: source contributions and meteorological influences, Atmospheric Chemistry and Physics, 19, 8339-8361, 2019.

Morrison, H., Thompson, G., and Tatarskii, V.: Impact of cloud microphysics on the development of trailing stratiform precipitation in a simulated squall line: Comparison of one-and two-moment schemes, Monthly weather review, 137, 991-1007, 2009.

Potter, P., Ramankutty, N., Bennett, E. M., and Donner, S. D.: Characterizing the spatial patterns of global fertilizer application and manure production, Earth interactions, 14, 1-22, 2010.

Tie, X., Li, G., Ying, Z., Guenther, A., and Madronich, S.: Biogenic emissions of isoprenoids and NO in China and comparison to anthropogenic emissions, Science of the total environment, 371, 238-251, 2006.
Wang, Q. g., Han, Z., and Higano, Y.: An inventory of nitric oxide emissions from soils in China, Environmental pollution, 135, 83-90, 2005.
Wang, R., Bei, N., Wu, J., Li, X., Liu, S., Yu, J., Jiang, Q., Tie, X., and Li, G.: Cropland nitrogen dioxide emissions and effects on the ozone pollution in the North China plain, Environmental Pollution, 294, 118617, 2022.
Wang, Y., McElroy, M. B., Martin, R. V., Streets, D. G., Zhang, Q., and Fu, T. M.: Seasonal variability of NO_x emissions over east China constrained by satellite observations: Implications for combustion and microbial sources, Journal of Geophysical Research: Atmospheres, 112, 2007.
Yan, X., Ohara, T., and Akimoto, H.: Statistical modeling of global soil NO_x emissions, Global Biogeochemical Cycles, 19, 2005.
Yarwood, G., Jung, J., Whitten, G. Z., Heo, G., Mellberg, J., and Estes, M.: Updates to the Carbon Bond mechanism for version 6 (CB6), 9th Annual CMAS Conference, Chapel Hill, NC, 11-13,
Zhang, L., Brook, J. R., and Vet, R.: A revised parameterization for gaseous dry deposition in air-quality models, Atmospheric Chemistry and Physics, 3, 2067-2082, 2003.